J. Fluid Mech. (1991), vol. 224, pp. 305–333
Printed in Great Britain

Electrophoresis of a colloidal sphere along the axis of a circular orifice or a circular disk

By HUAN J. KEH† AND LIANG C. LIEN
Department of Chemical Engineering, National Taiwan University, Taipei 10764 Taiwan, ROC

(Received 28 February 1990 and in revised form 24 August 1990)

The axisymmetric electrophoretic motion of a dielectric sphere along the axis of an orifice in a large conducting plane or of a conducting disk is considered. The radius of the orifice or the disk may be either larger or smaller than that of the sphere. The assumption of thin electrical double layers at the solid surfaces is employed. To solve the electrostatic and hydrodynamic governing equations both the electric and the flow fields are partitioned at the plane of the orifice or the disk. For each field, separate solutions are developed on both sides of the plane that satisfy the boundary conditions in each region and the unknown functions for the field at the fluid interface. The continuities of the electric current flux and the fluid stress tensor at the matching interface lead to sets of dual integral equations which are solved analytically to determine the unknown functions for the fields at the matching interface. Then, a boundary–collocation technique is used to satisfy the boundary conditions on the surface of the sphere.

The numerical solutions for the electrophoretic velocity of the colloidal sphere are presented for various values of a/b and a/d, where a is the particle radius, b is the radius of the orifice or the disk, and d is the distance of the particle centre from the plane of the wall. For the limiting case of electrophoresis of a sphere perpendicular to an infinite plane wall, our results for the boundary effects agree very well with the exact calculations using spherical bipolar coordinates. Interestingly, the electrophoretic velocity of a sphere approaching an orifice of a larger radius increases when the sphere is close to the orifice, and this velocity can be even larger than that for an identical sphere undergoing electrophoresis in an unbounded fluid. If the sphere has a radius larger than that of the orifice, or if the sphere has a smaller radius and is located sufficiently far from the orifice, its electrophoretic mobility will decrease with the increase of the spacing parameter a/d. For the electrophoretic motion of a sphere along the axis of and close to a disk of finite radius, the resistance to the particle movement can be stronger than that for an equal sphere undergoing electrophoresis normal to an infinite plane wall at the same value of a/d. As the particle approaches the disk wall, its mobility decreases steadily and vanishes at the limit $a/d \to 1$. The boundary effects on the particle mobility and the fluid flow pattern in electrophoresis differ significantly from those of the corresponding sedimentation problem with which a comparison is made.

1. Introduction

A charged particle suspended in an electrolyte solution is surrounded by a diffuse cloud of ions carrying a total charge equal and opposite in sign to that of the particle. This distribution of fixed charge and diffuse ions is known as an electrical double

† Author to whom correspondence should be sent.

layer. When an electric field is imposed on the particle, a force is exerted on both parts of the double layer. The particle is attracted toward the electrode of its opposite sign, while the ions in the diffuse layer migrate in the other direction. This particle's motion is called electrophoresis and has been applied to the particle characterization or separation in a variety of colloidal and biological systems.

The electrophoretic velocity $\boldsymbol{U}_0$ of an isolated particle is related to the applied electric field $\boldsymbol{E}_\infty$ by the Smoluchowski equation,

$$\boldsymbol{U}_0 = \frac{\epsilon\zeta}{4\pi\eta}\boldsymbol{E}_\infty. \tag{1.1}$$

Here, η and ϵ represent the viscosity coefficient and the dielectric constant, respectively, of the solution surrounding the particle, and ζ is the zeta potential associated with the particle surface. The ratio U_0/E_∞ is the electrophoretic mobility of the particle. Equation (1.1) applies to non-conducting particles of arbitrary shape, provided that the local radii of curvature of the particle are much larger than the thickness of the double layer surrounding the particle (Morrison 1970; Hunter 1987). On the other hand, the fluid velocity at the outer edge of the diffuse layer $\boldsymbol{v}_s$ relative to the particle's movement is related to the local electric field $\boldsymbol{E}_s$ by the Helmholtz expression for electro-osmotic flows:

$$\boldsymbol{v}_s = -\frac{\epsilon\zeta}{4\pi\eta}\boldsymbol{E}_s. \tag{1.2}$$

Here the subscript s denotes fields at the solid surface (more precisely, the outer boundary of the thin double layer), which have no normal components. In deriving (1.1) and (1.2), the particle has been treated as locally flat, and the effects of the polarization of interfacial ions have been neglected.

The Smoluchowski equation serves only for fluid media that extend to infinity in all directions. However, in practical applications of electrophoresis, colloidal particles are not isolated and will move in the presence of neighbouring particles and/or boundaries. Recently, much progress has been made in the mathematical analysis concerning the applicability of (1.1) for a charged particle surrounded by a thin double layer in a variety of bounded systems. Using a method of reflections, Chen & Keh (1988) analytically solved the problem of the electrophoretic motion of two arbitrarily oriented, freely suspended spheres with arbitrary ratios of radii and of zeta potentials. Corrections to Smoluchowski's equation due to particle interactions are determined in a power series of r_{12}^{-1} up to $O(r_{12}^{-7})$, where r_{12} is the centre-to-centre distance between the particles. Based on a microscopic model (Batchelor 1972; Reed & Anderson 1980; Anderson 1981), the interaction effects between pairs of particles were utilized to find the effect of particles' volume fraction on the average electrophoretic mobility in a bounded, dilute dispersion of rigid spheres with arbitrary size and/or zeta-potential distributions. The two-sphere problem of electrophoresis was also semi-analytically solved by Keh & Chen (1989*a*, *b*) using spherical bipolar coordinates. This work extended the earlier effort of Reed & Morrison (1976) from two non-rotating spheres of identical radii to two freely suspended spheres of arbitrary radii and provided convergent numerical solutions of the particle velocities for various separation distances between the particles. Using a boundary–collocation technique, Keh & Yang (1990) studied the axisymmetric electrophoretic motion of multiple spheres along their line of centres. In this analysis, the spheres may differ in radius and in zeta potential and they are allowed to be

unequally spaced. The numerical results of particle-interaction effects could be obtained with good convergence even when the particles are touching one another.

There are four important conclusions resulting from these investigations of the particle interactions in electrophoresis. First, the particle interaction effect on electrophoresis is in general much weaker than on sedimentation, because the disturbance to the fluid velocity field caused by an electrophoretic sphere decays faster (as r^{-3}) than that caused by a settling sphere (as r^{-1}), where r is the distance from the particle centre. Second, for the case of two spheres undergoing asymmetric electrophoretic motion, both particles rotate in the same direction, opposite to the case of two sedimenting spheres. Third, the influence on the interactions among particles in general is far greater on the smaller ones than on the larger ones. Fourth, the electrophoretic velocity of each particle is unaffected by the presence of the others if all of the particles in the suspension have the same zeta potential. The feature that there is no net effect of particle interactions in electrophoresis in an unbounded suspension of particles with identical zeta potential and thin double layer was also observed by using a unit cell model (Kozak & Davis 1989) and confirmed by a potential-flow reasoning (Anderson 1989; Acrivos, Jeffrey & Saville 1990).

In addition to the examinations of interaction effects among electrophoretic particles, the electrophoresis of a colloidal sphere in the proximity of fixed boundaries has also been theoretically studied in recent years. The electrophoretic motion of a sphere near an infinite plane wall, in a long circular tube, or along the centreline between two large parallel plates was investigated by Keh & Anderson (1985) using the method of reflections. The particle mobility was determined in a power series of λ up to $O(\lambda^6)$, where λ is the ratio of the particle radius to the distance between the particle centre and the boundary. Ignoring the $O(\lambda^0)$ electro-osmotic effect, the leading boundary effect is $O(\lambda^3)$, which is weak in comparison with the $O(\lambda)$ effect for sedimentation.

Utilizing bipolar coordinates, Keh & Chen (1988) obtained the exact solution for the problem of the electrophoresis of a freely suspended sphere parallel to a large non-conducting plane. The wall effect was found to impede the particle velocity for moderate to large separations; however, closer to the wall this velocity goes through a minimum at $\lambda \approx 0.77$ and then increases as $\lambda \to 1$, such that the particle moves faster when $\lambda \geqslant 0.91$ than it would at $\lambda \to 0$. Also, the electrophoretic particle rotates in the direction opposite to that which would occur for a solid sphere settling near a parallel wall. On the other hand, the electrophoretic migration of a sphere normal to an infinite conducting plane was studied by Morrison & Stukel (1970) and the present authors (Keh & Lien 1989) using bipolar coordinates. In this case, the particle mobility decreases monotonically as the particle approaches the wall and goes to zero in the limit of $\lambda \to 1$.

All previous solutions for the wall-corrected electrophoretic velocity of a sphere have involved infinite planar or cylindrical surfaces. In this paper we examine the axisymmetric electrophoretic motion of an insulating sphere along the axis of an orifice in a large conducting plane or of a conducting disk with a finite radius. The assumption of thin double layers adjacent to solid surfaces is employed throughout the analysis. The combined analytical–numerical procedure with a boundary-collocation technique, similar to that described in Dagan, Pfeffer & Weinbaum (1982*a*) and Dagan, Weinbaum & Pfeffer (1982*c*), is used to solve the quasi-steady electrostatic and momentum equations applicable to the system. Corrections to the Smoluchowski equation for the particle velocity are obtained with good convergence and the streamlines for fluid motion are presented for various cases. For the limiting

case of electrophoresis towards an orifice of zero opening area or a disk of infinite radius, our numerical results for the particle mobility show excellent agreement with the exact solution obtained by using bipolar coordinates.

The paper is presented in six sections. In §2 the problem of electrophoretic motion of a sphere along the axis of an orifice is formulated and its solution scheme is furnished. Based on this analysis, the numerical solutions for the movement of a sphere towards an orifice are obtained in §3. Section 4 contains the formulation and manipulations of a complementary problem to that treated in §2, the electrophoresis of a sphere along the axis of a disk. The numerical results for the disk-corrected velocity of the particle and their discussion are given in §5.

2. Formulation for the electrophoretic motion of a sphere toward an orifice

In this section we consider the axisymmetric electrophoretic motion of a non-conducting sphere of radius a towards a circular orifice of radius b in a perfectly conducting plane of zero thickness whose distance from the sphere is d, as shown in figure 1. Here, (ρ, ϕ, z) and (r, θ, ϕ) denote the circular cylindrical and the spherical coordinates, respectively, and the origin of coordinates is chosen at the sphere centre. The uniformly applied electric field is expressed by $E_\infty \boldsymbol{e}_z$, where $\boldsymbol{e}_z$ is a unit vector in z-direction. The following analysis is valid up to the point where the sphere is tangent to the plane of the orifice. The thickness of electrical double layers is assumed to be small relative to the radius of the sphere and to the surface-to-surface spacing between the particle and the orifice wall. Gravitational effects are ignored. The objective is to determine the correction to Smoluchowski's equation (1.1) for the particle due to the presence of the plane of the orifice.

Before determining the electrophoretic velocity for the particle, the electrical potential and fluid velocity fields outside the particle must be solved.

2.1. *Electrical potential distribution*

The fluid outside the thin double layer is electrically neutral and is assumed to be of constant conductivity; hence, the electrical potential distribution $\Phi(\boldsymbol{x})$ is governed by Laplace's equation:

$$\nabla^2 \Phi = 0. \tag{2.1}$$

The local electric field $\boldsymbol{E}(\boldsymbol{x})$ equals $-\nabla\Phi$. The potential gradient far away from the particle approaches the undisturbed applied electric field and the normal component of the current flux at the surface of the insulating particle vanishes. Thus, the electrical potential is subject to the following boundary conditions:

$$\frac{\partial \Phi}{\partial r} = 0 \qquad \text{at} \qquad r = a, \tag{2.2a}$$

$$\Phi = -E_\infty d \quad \text{at} \quad z = d \text{ and } b \leqslant \rho < \infty, \tag{2.2b}$$

$$\Phi \to -E_\infty z \quad \text{as} \quad r \to \infty. \tag{2.2c}$$

The potential on the conducting plane of the orifice has been set equal to $-E_\infty d$ for convenience.

To solve (2.1) and (2.2) we divide the potential field into two simply bounded regions: the half-space containing the sphere and bounded by the orifice wall, $z \leqslant d$, and the remaining infinite half-space, $z \geqslant d$. This partitioning of the electric field establishes well-defined regions in which the solution for the potential distribution

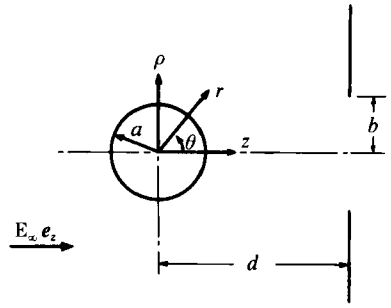

FIGURE 1. Electrophoresis of a spherical particle along the axis of a circular orifice in an infinite conducting plane of zero thickness.

can be obtained in terms of the unknown potential profile at the orifice opening. The essential mathematical problem is to match the solution in each region at the orifice opening to secure continuity of the potential and electric fields. This solution procedure was employed by Dagan *et al.* (1982*c*) to study the creeping motion of a sphere along the axis of an orifice.

Since the governing equation and boundary conditions are linear, one can write the potential distribution Φ^{I} for the region $z \leqslant d$ as the superposition

$$\Phi^{\mathrm{I}} = \Phi_{\mathrm{w}} + \Phi_{\mathrm{s}}. \tag{2.3}$$

Here, Φ_{w} is a solution of (2.1) in cylindrical coordinates that represents the disturbances produced by the orifice and the wall approaching the plane $z = d$ from the left plus the undisturbed applied electric potential and is given by

$$\Phi_{\mathrm{w}} = -E_\infty z + \int_0^\infty \omega R_1(\omega)\, J_0(\omega\rho)\, \mathrm{e}^{\omega z}\, \mathrm{d}\omega, \tag{2.4}$$

where J_0 is the Bessel function of the first kind of order zero and $R_1(\omega)$ is an unknown function of ω. The second term on the right-hand side of (2.3), Φ_{s}, is a solution of (2.1) in spherical coordinates representing the disturbances generated by the sphere and is given by

$$\Phi_{\mathrm{s}} = \sum_{n=0}^{\infty} T_n\, r^{-(n+1)} P_n(\cos\theta), \tag{2.5}$$

where P_n is the Legendre polynomial of order n and T_n are unknown constant coefficients.

For the region $z \geqslant d$, it is sufficient to represent all disturbances generated at the plane $z = d$ by a Fourier–Bessel integral of the form given by (2.4),

$$\Phi^{\mathrm{II}} = -E_\infty z + \int_0^\infty \omega R_2(\omega)\, J_0(\omega\rho)\, \mathrm{e}^{-\omega z}\, \mathrm{d}\omega, \tag{2.6}$$

where $R_2(\omega)$ is an unknown function of ω. Note that a solution of the forms of Φ^{I} and Φ^{II} given by (2.3)–(2.6) immediately satisfies boundary condition (2.2*c*).

A brief conceptual summary of the solution procedure to determine $R_1(\omega)$, $R_2(\omega)$ and T_n is given below to help the readers follow the mathematical development. At first, boundary condition (2.2*b*) is satisfied along the orifice wall in each region. This permits the unknown function $R_1(\omega)$ to be determined in terms of the coefficients T_n and the unknown potential profile at the opening of the orifice. Similarly, $R_2(\omega)$ can be determined in terms of the unknown potential at the orifice opening. Then, by matching the current flux at the orifice opening, the unknown orifice potential can

be obtained in terms of the coefficients T_n. Finally, boundary condition (2.2a) on the surface of the sphere can be satisfied by making use of the collocation method and the solution of the collocation matrix provides numerical values for the coefficients T_n. This solution procedure is valid up to the point where the sphere is tangent to the plane of the orifice.

The electrical potential profile at the orifice opening can be defined in a general form by

$$\Phi(\rho, d) = -E_\infty d + \frac{h(\rho)}{\rho} \quad (0 \leqslant \rho < b). \tag{2.7}$$

In the plane $z = d$, the potential equals $-E_\infty d$ for $\rho \geqslant b$ and the potential and the current flux are continuous for $\rho < b$. Thus the boundary conditions at the matching plane are mixed:

$$\Phi^{\mathrm{I}}(\rho, d) = \Phi^{\mathrm{II}}(\rho, d) = \begin{cases} -E_\infty d & (b \leqslant \rho < \infty) \\ -E_\infty d + \dfrac{h(\rho)}{\rho} & (0 \leqslant \rho < b), \end{cases} \tag{2.8}$$

$$\frac{\partial \Phi^{\mathrm{I}}}{\partial z}(\rho, d) = \frac{\partial \Phi^{\mathrm{II}}}{\partial z}(\rho, d) \quad (0 \leqslant \rho < b). \tag{2.9}$$

Substitution of the solution Φ^{I} given by (2.3)–(2.5) into the boundary condition (2.8) and application of Hankel transforms on the variable ρ lead to a solution for $R_1(\omega)$ in terms of the unknown coefficients T_n and the unknown potential function $h(\rho)$. The resulting potential field in the half-space containing the sphere is given by

$$\Phi^{\mathrm{I}} = -E_\infty z + \int_0^\infty h^*(\omega) J_0(\omega\rho) \, \mathrm{e}^{-\omega(d-z)} \, \mathrm{d}\omega + \sum_{n=0}^{\infty} T_n [B_n''(\rho, z) - B_n''(\rho, 2d - z)], \tag{2.10}$$

where

$$h^*(\omega) = \omega \int_0^b h(t) J_0(\omega t) \, \mathrm{d}t, \tag{2.11}$$

and $B_n''(\rho, z)$ is defined by (A 7) in the Appendix. It is easy to show that

$$\int_0^\infty h^*(\omega) J_0(\omega\rho) \, \mathrm{d}\omega = 0 \quad (b \leqslant \rho < \infty). \tag{2.12}$$

Following a similar procedure, the boundary condition (2.8) can be satisfied by Φ^{II} in the form of (2.6) for the half-space $z \geqslant d$ and $R_2(\omega)$ can be expressed in terms of the unknown function $h(\rho)$ for the potential at the orifice. Substituting this result for $R_2(\omega)$ into (2.6) one obtains

$$\Phi^{\mathrm{II}} = -E_\infty z + \int_0^\infty h^*(\omega) J_0(\omega\rho) \, \mathrm{e}^{\omega(d-z)} \, \mathrm{d}\omega. \tag{2.13}$$

Although the potentials in (2.10) and (2.13) are still expressed in terms of the unknown coefficients T_n and the unknown function h, they do satisfy the boundary conditions (2.2b) and (2.2c) and can properly represent any arbitrary potential profile at the orifice opening.

Application of the matching condition (2.9) to (2.10) and (2.13) results in

$$\int_0^\infty \omega h^*(\omega) J_0(\omega\rho) \, \mathrm{d}\omega = H(\rho) \quad (0 \leqslant \rho < b), \tag{2.14a}$$

where

$$H(\rho) = \frac{1}{2} \sum_{n=0}^{\infty} T_n [(n+1) B_{n+1}''(\rho, d) + \int_0^\infty \frac{\omega^{n+1}}{n!} J_0(\omega\rho) \, \mathrm{e}^{-\omega d} \, \mathrm{d}\omega]. \tag{2.14b}$$

Equations (2.14*a*) and (2.12) comprise a set of dual integral equations for the function $h^*(\omega)$. The solution of these dual integral equations follows from the results of Tranter (1951), yielding

$$h^*(\omega) = \frac{2}{\pi}\int_0^b \mathrm{d}t \sin\omega t \int_0^t \mathrm{d}s \frac{s}{(t^2-s^2)^{\frac{1}{2}}} H(s)$$

$$= \frac{2}{\pi}\sum_{n=0}^{\infty} T_n \int_0^b S_{n+1}(t,d)\sin\omega t\,\mathrm{d}t, \tag{2.15}$$

where the definition of $S_n(t,d)$ is given by (A 13).

The result for $h^*(\omega)$ is substituted back into (2.10) and (2.13) and the electrical potential distribution for the two semi-infinite spaces is obtained:

$$\Phi^{\mathrm{I}} = -E_\infty z + \sum_{n=0}^{\infty} T_n\left[B_n''(\rho,z) - B_n''(\rho,2d-z) + \frac{2}{\pi}\int_0^b S_{n+1}(t,d)\,K_0^0(\rho,z,t)\,\mathrm{d}t\right], \tag{2.16a}$$

$$\Phi^{\mathrm{II}} = -E_\infty z + \sum_{n=0}^{\infty} T_n \frac{2}{\pi}\int_0^b S_{n+1}(t,d)\,K_0^0(\rho,z,t)\,\mathrm{d}t, \tag{2.16b}$$

where $K_\nu^\mu(\rho,z,t)$ is defined by (A 14). Equation (2.16) provides an exact solution for the potential at the orifice opening and the unknown coefficients T_n must be determined from the remaining boundary condition (2.2*a*) on the surface of the sphere. It should be noted that in the limiting case of an orifice with zero radius (i.e. an infinite plane wall), $h(\rho) = h^*(\omega) = 0$ and the resulting solution for the potential field is

$$\Phi^{\mathrm{I}} = -E_\infty z + \sum_{n=0}^{\infty} T_n[B_n''(\rho,z) - B_n''(\rho,2d-z)]. \tag{2.17}$$

Utilizing the relation

$$\frac{\partial}{\partial r} = \sin\theta\frac{\partial}{\partial\rho} + \cos\theta\frac{\partial}{\partial z}, \tag{2.18}$$

one can apply (2.2*a*) to (2.16) to yield

$$\sum_{n=0}^{\infty} T_n\left\{\rho[A_n(\rho,z) - A_n(\rho,2d-z)] - (n+1)\,z[B_{n+1}''(\rho,z) + B_{n+1}''(\rho,2d-z)]\right.$$

$$\left. + \frac{2}{\pi}\left[z\int_0^b S_{n+1}(t,d)\,K_0^1(\rho,z,t)\,\mathrm{d}t - \rho\int_0^b S_{n+1}(t,d)\,K_1^1(\rho,z,t)\,\mathrm{d}t\right]\right\} = E_\infty z \quad (r=a), \tag{2.19}$$

where $$A_n(\rho,z) = \frac{nz^2-(n+1)\rho^2}{\rho(\rho^2+z^2)^{\frac{1}{2}(n+3)}} P_n\left[\frac{z}{(\rho^2+z^2)^{\frac{1}{2}}}\right] - \frac{nz}{\rho(\rho^2+z^2)^{\frac{1}{2}(n+2)}} P_{n-1}\left[\frac{z}{(\rho^2+z^2)^{\frac{1}{2}}}\right]. \tag{2.20}$$

The definite integrals in (2.19) must be performed numerically.

To satisfy the condition (2.19) exactly along the entire semicircular generating arc of the sphere would require the solution of the entire infinite array of unknown coefficients T_n. However, the collocation technique (O'Brien 1968; Gluckman, Pfeffer & Weinbaum 1971; Dagan *et al.* 1982*c*; Keh & Yang 1990) enforces the boundary condition at a finite number of discrete points on the sphere's generating arc and truncates the infinite series (2.16) into a finite one. The unknown coefficient in each term of the series permits one to satisfy the exact boundary condition at one discrete point on the sphere surface. Thus, if the spherical boundary is approximated by satisfying condition (2.2*a*) at N discrete points on its generating arc, the infinite series

in (2.16) is truncated after N terms, resulting in a system of N simultaneous linear algebraic equations in the truncated form of (2.19). This matrix equation can be solved by any of the standard matrix-reduction techniques to yield the N unknown coefficients T_n required in the truncated equation of (2.16) for the electrical potential distribution. The accuracy of the truncation technique can be improved to any degree by taking a sufficiently large value of N. Naturally, as $N \to \infty$ the truncation error vanishes and the overall accuracy of the solution depends only upon the numerical integration required in evaluating the matrix elements.

2.2. *Fluid velocity distribution*

Having obtained a solution for the electrical potential distribution, we can now proceed to find the fluid velocity field. Because the Reynolds numbers of electrokinetic flows are small, the fluid motion outside the thin double layers is governed by the quasi-steady fourth-order differential equation for viscous axisymmetric flows,

$$\mathrm{E}^4\Psi = \mathrm{E}^2(\mathrm{E}^2\Psi) = 0, \tag{2.21}$$

in which the Stokes stream function Ψ is related to the velocity components in cylindrical coordinates by

$$v_\rho = \frac{1}{\rho}\frac{\partial \Psi}{\partial z}, \qquad v_z = -\frac{1}{\rho}\frac{\partial \Psi}{\partial \rho}, \tag{2.22a, b}$$

and the operator E^2 has the form

$$\mathrm{E}^2 = \rho\frac{\partial}{\partial \rho}\left(\frac{1}{\rho}\frac{\partial}{\partial \rho}\right) + \frac{\partial^2}{\partial z^2}. \tag{2.23}$$

Since the electric field acting on the diffuse ions within the double layer at the particle surface produces a relative tangential fluid velocity at the outer edge of the double layer (apparent surface 'slip velocity') as given by (1.2) and the fluid is motionless at the conducting plane of orifice and far away from the particle, the boundary conditions for the velocity field are

$$\boldsymbol{v} = U\boldsymbol{e}_z + \frac{\epsilon\zeta}{4\pi\eta}\nabla\Phi \quad \text{at} \quad r = a, \tag{2.24a}$$

$$\boldsymbol{v} = \boldsymbol{0} \quad \text{at} \quad z = d \text{ and } b \leqslant \rho < \infty, \tag{2.24b}$$

$$\boldsymbol{v} = \boldsymbol{0} \quad \text{as} \quad r \to \infty, \tag{2.24c}$$

where ζ is the zeta potential of the particle surface and U is the instantaneous electrophoretic velocity of the particle to be determined. Note that the normal component of $\nabla\Phi$ vanishes at the particle surface as required by (2.2a) and the angular dependence of the tangential electric field is obtained from the potential distribution given by (2.16) with coefficients determined from (2.19).

Because the particle is freely suspended in the fluid and the particle 'surface' (which means the outer limit of the double layer) encloses a neutral body, the external fields produce no net force on the particle. Thus, the constraint of zero drag force exerted by the fluid on the particle surface must be satisfied,

$$\boldsymbol{F} = \iint_{r=a} \boldsymbol{e}_r \cdot \boldsymbol{\Pi}\, \mathrm{d}S = \boldsymbol{0}, \tag{2.25}$$

where $\boldsymbol{\Pi}$ is the fluid stress tensor and $\boldsymbol{e}_r$ is the unit vector in the radial direction. For the axisymmetric motion considered in this section, the sphere translates without rotation and one can evaluate U by satisfying (2.25) after solving (2.21) and (2.24).

In view of the linearity of the governing equation (2.21) and the boundary conditions (2.24), the total flow can be decomposed into two contributions. First we consider the fluid motion about a sphere translating along the axis of an orifice with velocity $U\boldsymbol{e}_z$. The Stokes equations for this flow were solved by Dagan *et al.* (1982*c*). They obtained the stream function (Ψ_1) for the flowing fluid and determined that the force exerted by the fluid on the particle can be written in the form

$$F_1 = -6\pi\eta a U\alpha, \tag{2.26}$$

where α is the correction factor to Stokes' law due to the presence of the orifice wall. The value of α depends upon the ratios a/b and a/d and can be numerically computed using the boundary–collocation method. A first-order approximate solution for α has been obtained analytically by Davis, O'Neill & Brenner (1981).

We now consider the fluid flow caused by a stationary sphere situated on the axis of an orifice with a tangential electrokinetic velocity at the particle 'surface', prescribed by (2.24*a*) with U equal to zero; namely, the boundary conditions at the particle surface become

$$\left.\begin{aligned} v_{2\rho} &= \frac{\epsilon\zeta}{4\pi\eta}\frac{\partial\Phi}{\partial\rho} \\ v_{2z} &= \frac{\epsilon\zeta}{4\pi\eta}\frac{\partial\Phi}{\partial z} \end{aligned}\right\} \text{at} \quad r = a. \tag{2.27}$$

Superposition of this velocity field upon that formerly considered, caused by a sphere translating towards an orifice, yields the total fluid velocity field generated by the electrophoretic motion of a non-conducting sphere along the axis of a circular orifice. By obtaining the force F_2 acting on the stationary sphere, adding it to F_1 given by (2.26) and equating the sum to zero, Smoluchowski's equation with wall corrections will result.

To find the drag force acting on the stationary sphere with a tangential velocity distribution at the surface, we divide the flow field into two regions just as we did for the electrical potential field. The stream function for the region $z \leqslant d$ is linearly composed of two parts:

$$\Psi_2^{\mathrm{I}} = \Psi_{\mathrm{w}} + \Psi_{\mathrm{s}}. \tag{2.28}$$

Here Ψ_{w} is a solution of (2.21) in cylindrical coordinates that represents the disturbances produced by the orifice and the wall and is given by a Fourier–Bessel integral,

$$\Psi_{\mathrm{w}} = \int_0^\infty \rho J_1(\omega\rho)\,[X_1(\omega) + zY_1(\omega)]\,\mathrm{e}^{\omega z}\,\mathrm{d}\omega, \tag{2.29}$$

where J_1 is the Bessel function of the first kind of order one and $X_1(\omega)$ and $Y_1(\omega)$ are unknown functions of ω. The second part of Ψ_2^{I}, denoted by Ψ_{s} is a solution of (2.21) in spherical coordinates representing the disturbances generated by the sphere and is given by the summation of a multipole series

$$\Psi_{\mathrm{s}} = \sum_{n=2}^{\infty} (B_n r^{-n+1} + D_n r^{-n+3})\, G_n^{-\frac{1}{2}}(\cos\theta), \tag{2.30}$$

where $G_n^{-\frac{1}{2}}$ is the Gegenbauer polynomial of the first kind of order n and degree $-\frac{1}{2}$; B_n and D_n are unknown constant coefficients.

For the semi-infinite region $z \geqslant d$, an integral similar to the form of (2.29) is chosen for the stream function to represent the disturbances generated at the plane of the orifice,

$$\Psi_2^{\mathrm{II}} = \int_0^\infty \rho J_1(\omega\rho)\,[X_2(\omega) + zY_2(\omega)]\,\mathrm{e}^{-\omega z}\,\mathrm{d}\omega. \tag{2.31}$$

Here $X_2(\omega)$ and $Y_2(\omega)$ are unknown functions of ω. Note that the boundary condition (2.24*c*) is immediately satisfied by a solution of the forms of Ψ_2^{I} and Ψ_2^{II} given by (2.28)–(2.31).

The velocity components at the orifice opening can be defined in a general form by

$$v_{2z}(\rho,d)=f(\rho)/\rho, \quad v_{2\rho}(\rho,d)=-g(\rho)/\rho \qquad (0\leqslant\rho<b). \tag{2.32}$$

The kinematic boundary conditions in the matching plane $z=d$ require that the velocity vanish for $\rho\geqslant b$ and that the velocity be continuous for $\rho<b$; namely,

$$v_{2z}^{\mathrm{I}}(\rho,d)=v_{2z}^{\mathrm{II}}(\rho,d)=\begin{cases}0 & (b\leqslant\rho<\infty)\\ f(\rho)/\rho & (0\leqslant\rho<b),\end{cases} \tag{2.33a}$$

$$v_{2\rho}^{\mathrm{I}}(\rho,d)=v_{2\rho}^{\mathrm{II}}(\rho,d)=\begin{cases}0 & (b\leqslant\rho<\infty)\\ -g(\rho)/\rho & (0\leqslant\rho<b).\end{cases} \tag{2.33b}$$

In addition, the dynamic matching of the two flow fields require that the stress tensor be continuous at the orifice opening. This condition can be replaced by matching the pressure and its gradient for $\rho<b$ (Dagan, Weinbaum & Pfeffer 1982*b*):

$$P^{\mathrm{I}}(\rho,d)=P^{\mathrm{II}}(\rho,d), \quad \frac{\partial P^{\mathrm{I}}}{\partial z}(\rho,d)=\frac{\partial P^{\mathrm{II}}}{\partial z}(\rho,d). \tag{2.34a, b}$$

The expression for the pressure field in each region can be determined by integrating the following relation with the appropriate stream function representation:

$$\frac{\partial P}{\partial z}=-\frac{\eta}{\rho}\frac{\partial}{\partial\rho}(\mathbf{E}^2\Psi). \tag{2.35}$$

Note that $P^{\mathrm{I}}(z\to-\infty)=P^{\mathrm{II}}(z\to\infty)$ for the fluid motion.

Application of the boundary conditions (2.33) to (2.28)–(2.31) using (2.22) leads to solutions for $X_1(\omega)$, $Y_1(\omega)$, $X_2(\omega)$ and $Y_2(\omega)$ in terms of the unknown coefficients B_n and D_n as well as the unknown velocity functions $f(\rho)$ and $g(\rho)$. Furthermore, the functions $f(\rho)$ and $g(\rho)$ can be solved in terms of the coefficients B_n and D_n by utilizing the pressure matching conditions (2.34). After considerable algebraic manipulation the velocity components for the region $z\leqslant d$ are obtained in the form (Dagan *et al.* 1982*c*)

$$v_{2\rho}^{\mathrm{I}}=\sum_{n=2}^{\infty}\left\{B_n\left[\beta_n'(\rho,z)+\frac{2}{\pi}\int_0^b\beta_n^*(\rho,z,t)\,\mathrm{d}t\right]+D_n\left[\delta_n'(\rho,z)+\frac{2}{\pi}\int_0^b\delta_n^*(\rho,z,t)\,\mathrm{d}t\right]\right\}, \tag{2.36a}$$

$$v_{2z}^{\mathrm{I}}=\sum_{n=2}^{\infty}\left\{B_n\left[\beta_n''(\rho,z)+\frac{2}{\pi}\int_0^b\beta_n^{**}(\rho,z,t)\,\mathrm{d}t\right]+D_n\left[\delta_n''(\rho,z)+\frac{2}{\pi}\int_0^b\delta_n^{**}(\rho,z,t)\,\mathrm{d}t\right]\right\}, \tag{2.36b}$$

where the functions β_n', β_n'', δ_n', δ_n'', β_n^*, β_n^{**}, δ_n^* and δ_n^{**} are defined by (A 1)–(A 14). The velocity components for the other half-space ($z\geqslant d$) are

$$v_{2\rho}^{\mathrm{II}}=\sum_{n=2}^{\infty}\left\{B_n\frac{2}{\pi}\int_0^b\beta_n^*(\rho,z,t)\,\mathrm{d}t+D_n\frac{2}{\pi}\int_0^b\delta_n^*(\rho,z,t)\,\mathrm{d}t\right\}, \tag{2.36c}$$

$$v_{2z}^{\mathrm{II}}=\sum_{n=2}^{\infty}\left\{B_n\frac{2}{\pi}\int_0^b\beta_n^{**}(\rho,z,t)\,\mathrm{d}t+D_n\frac{2}{\pi}\int_0^b\delta_n^{**}(\rho,z,t)\,\mathrm{d}t\right\}. \tag{2.36d}$$

Although the velocity field in (2.36) is still expressed in terms of the unknown coefficients B_n and D_n, it does satisfy the boundary condition (2.24*b*) on the orifice wall and provide an exact solution for the velocity at the orifice opening. For the limiting case of an orifice with zero radius, $f(\rho) = g(\rho) = 0$ and (2.36*a*, *b*) can be simplified to become

$$v_{2\rho}^{\mathrm{I}} = \sum_{n=2}^{\infty} [B_n \beta_n'(\rho, z) + D_n \delta_n'(\rho, z)], \quad v_{2z}^{\mathrm{I}} = \sum_{n=2}^{\infty} [B_n \beta_n''(\rho, z) + D_n \delta_n''(\rho, z)]. \tag{2.37a, b}$$

The only boundary conditions that remain to be satisfied are those on the sphere surface. Substituting (2.16*a*) into (2.27) one obtains the tangential fluid velocity at the particle 'surface':

$$v_{2\rho}|_{r=a} = \frac{\epsilon\zeta}{4\pi\eta} \sum_{n=0}^{\infty} T_n \left\{ A_n(\rho, z) - A_n(\rho, 2d-z) - \frac{2}{\pi} \int_0^b S_{n+1}(t, d)\, K_1^1(\rho, z, t)\, \mathrm{d}t \right\}, \tag{2.38a}$$

$$v_{2z}|_{r=a} = -\frac{\epsilon\zeta}{4\pi\eta} E_\infty - \frac{\epsilon\zeta}{4\pi\eta} \sum_{n=0}^{\infty} T_n \left\{ (n+1)\,[B_{n+1}''(\rho, z) + B_{n+1}''(\rho, 2d-z)] \right.$$
$$\left. - \frac{2}{\pi} \int_0^b S_{n+1}(t, d)\, K_0^1(\rho, z, t)\, \mathrm{d}t \right\}. \tag{2.38b}$$

Here the first N coefficients T_n have been determined through the procedure given in §2.1. Application of these boundary conditions to (2.36*a*, *b*) can be accomplished by utilizing the collocation technique presented for the solution of the electrical potential field. At $r = a$, boundary conditions (2.38) are applied at M discrete points and the series solution (2.36) is truncated after M terms. This generates a set of $2M$ linear algebraic equations for the $2M$ unknown coefficients B_n and D_n. The fluid velocity field is completely solved once these coefficients are determined. Note that the definite integrals in (2.36) and (2.38) must be performed numerically.

The drag force exerted by the fluid on the spherical boundary $r = a$ can be determined from (Happel & Brenner 1983)

$$F_2 = \eta\pi \int_0^\pi r^3 \sin^3\theta \frac{\partial}{\partial r}\left(\frac{\mathrm{E}^2\Psi}{r^2 \sin^2\theta}\right) r\, \mathrm{d}\theta. \tag{2.39}$$

Substitution of (2.28)–(2.30) into the above integral and application of the orthogonality properties of the Gegenbauer polynomials result in the simple relation

$$F_2 = 4\pi\eta D_2. \tag{2.40}$$

Equation (2.40) shows that only the first multipole contributes to the drag force exerted on the particle. Thus, the truncation procedure, which provides only an approximation to the actual boundary shape of the sphere, does not affect the drag result if the obtained value of D_2 is unchanged from its exact value.

2.3. *Derivation of the particle velocity*

Since the net force acting on the electrophoretic particle must vanish to satisfy the requirement of (2.25), one has

$$F_1 + F_2 = 0. \tag{2.41}$$

Substitution of the individual forces given by (2.26) and (2.40) yields the particle velocity

$$U = \frac{2D_2}{3a\alpha}. \tag{2.42}$$

Clearly, the ratio of the two forces F_1 and F_2 determines the electrophoretic mobility of the particle. By the linearity of the problem, the magnitude of the particle velocity is independent of the direction of travel.

3. Solutions for the electrophoretic motion of a sphere toward an orifice

The solution for the electrophoretic motion of a non-conducting sphere along the axis of an orifice, using the collocation technique described in the previous section, will be presented in this section. The results for the limiting case as $a/b \to \infty$ will be compared with the exact solution obtained by Keh & Lien (1989) for the electrophoresis of a sphere normal to an infinite conducting plane. (There is an error in equation (29) of Morrison & Stukel's (1970) analysis for this limiting case. It is likely that, because of this error, they failed to produce tabulated numerical results for the electrophoretic mobility of the particle.) The system of linear algebraic equations to be solved for coefficients T_n is constructed from (2.16a) and the boundary condition (2.19), while that for B_n and D_n is composed of (2.36a, b) and (2.38). When the sphere is migrating towards a plane wall, (2.16a) and (2.36a, b) are simplified to (2.17) and (2.37) and the definite integrals in (2.19) and (2.38) vanish.

When specifying the points along the semicircular generating arc of the sphere where the boundary conditions are to be exactly satisfied, the first point that should be chosen is $\theta = \frac{1}{2}\pi$, since this point defines the projected area of the sphere normal to the direction of motion. In addition, the points $\theta = 0$ and $\theta = \pi$ are important because they control the gap between the sphere and the plane at $z = d$. However, an examination of the systems of linear algebraic equations (2.19) as well as (2.36a, b) and (2.38) shows that the coefficient matrices become singular if these points are used. To overcome the difficulty of singularity and to preserve the geometric symmetry of the spherical boundary about the equatorial plane $\theta = \frac{1}{2}\pi$, points at $\theta = \alpha, \frac{1}{2}\pi - \alpha, \frac{1}{2}\pi + \alpha$ and $\pi - \alpha$ are taken to be four basic collocation points. Additional points along the boundary are selected as mirror-image pairs about the plane $\theta = \frac{1}{2}\pi$ to divide the two quarter-arcs of the sphere (more precisely, arcs with radian $\pi/2 - 2\alpha$) into equal segments. The optimum value of α in this work is found to be 0.01°, with which the numerical results of the particle velocity can converge to at least four significant digits for any ratios of particle-to-orifice radii a/b with a/d up to 0.9.

Numerical values of the wall-corrected reduced electrophoretic mobility for a sphere moving along the axis of a relatively small orifice (with $a/b = 10$) for various spacings are presented in the first and second columns of table 1. The corresponding numerical solutions for the electrophoresis of a sphere perpendicular to an infinite plane wall are given in the third column of the same table. All of the results obtained under this collocation scheme converge to at least five significant figures. The accuracy of the truncation technique is principally a function of the relative spacing a/d. For the difficult case of $a/d = 0.9$ (for $a/b = 10$) and $a/d = 0.99$ (for $a/b \to \infty$), the numbers of collocation points $N = 72$ and $M = 60$ are sufficiently large to achieve this convergence. The solutions for the electrophoretic motion of a sphere normal to a conducting plane obtained by using spherical bipolar coordinates (Keh & Lien 1989) are also listed in the last column of table 1 for a comparison. It can be found that the results from the collocation technique agree remarkably well with the exact results for all relative spacings between the sphere and the plane wall. The electrophoretic mobility of a sphere moving along the axis of an orifice with a relatively small radius is, as expected, in perfect agreement with that for a sphere

$\frac{a}{d}$	$\frac{4\pi\eta U}{\epsilon\zeta E_\infty}$		
	Orifice with $a/b = 10$ collocation technique	Infinite plane collocation technique	Infinite plane bipolar coordinates
0.1	0.99938	0.99938	0.99938
0.2	0.99504	0.99504	0.99504
0.3	0.98330	0.98330	0.98330
0.4	0.96022	0.96020	0.96020
0.5	0.92098	0.92089	0.92089
0.6	0.85898	0.85862	0.85862
0.7	0.76429	0.76297	0.76297
0.8	0.62170	0.61631	0.61631
0.9	0.40884	0.38584	0.38584
0.95	—	0.21993	0.21993
0.97	—	0.13979	0.13979
0.98	—	0.09605	0.09608
0.99	—	0.04979	0.04960

TABLE 1. The normalized electrophoretic mobilities for the motion of a sphere along the axis of an orifice with the ratio of radii $a/b = 10$ and for the motion of a sphere normal to an infinite plane

migrating toward an infinite plane wall unless the gap thickness between the sphere and the wall is very small. This agreement demonstrates the accuracy of the numerical solution obtained using the collocation technique.

The numerical results for the normalized electrophoretic mobility for various dimensionless sphere radii and sphere-to-wall spacings are presented in the first three columns of table 2 and plotted in figure 2. For the motion of a sphere on which a constant body force $\boldsymbol{Fe}_z$ (e.g. a gravitational field) is applied along the axis of a thin orifice, the particle velocity was obtained by using the point-force approximation (Davis *et al.* 1981) and the boundary–collocation technique (Dagan *et al.* 1982*c*). The Stokes-law correction for the sphere with various ratios of a/b and a/d has been computed and the collocation results are given in the last column of table 2 for comparison. Examination of the data shown in table 2 and figure 2 reveals an interesting feature. Both of the electrophoretic and hydrodynamic mobilities for a sphere whose radius is smaller than that of the orifice increase when the sphere is close to the orifice. Moreover, the electrophoretic mobility for a sphere near the opening can even be greater than that for an identical sphere undergoing electrophoresis in an unbounded medium. The reason that the electrophoretic velocity of the particle can be enhanced by the neighbouring orifice is partly due to the decreasing effective wall-interaction area that offers hydrodynamic resistance to the motion of a small sphere as it approaches the opening; the numerical results for the Stokes-law correction demonstrate this effect. However, a normalized electrophoretic mobility greater than unity is only possible because of the crowding of the electric field lines when they squeeze between the sphere and the orifice edge, which increases the local electrical force driving the particles' motion (Keh & Chen 1988). In figure 3, the electric field lines for the case of $a/b = 0.75$ and $a/d = 0.9$ are exhibited. The local electric field at the sphere 'surface' on the near side to the plane of the orifice appears to be enhanced in comparison with that on the far side. Obviously, the influence of this enhancement on the particle velocity can be very

$\frac{a}{b}$	$\frac{a}{d}$	Electrophoresis $\frac{4\pi\eta U}{\epsilon\zeta E_\infty}$	Sedimentation $\frac{6\pi\eta aU}{F}$
0.5	0.1	0.9994	0.890
	0.2	0.997	0.799
	0.3	0.994	0.746
	0.4	0.996	0.724
	0.5	1.001	0.718
	0.6	1.007	0.719
	0.7	1.013	0.721
	0.8	1.018	0.724
	0.9	1.021	0.726
1.0	0.1	0.9994	0.888
	0.2	0.995	0.782
	0.3	0.986	0.687
	0.4	0.973	0.611
	0.5	0.961	0.554
	0.6	0.954	0.513
	0.7	0.955	0.483
	0.8	0.963	0.459
	0.9	0.977	0.439
2.0	0.1	0.9994	0.888
	0.2	0.995	0.779
	0.3	0.984	0.674
	0.4	0.963	0.576
	0.5	0.930	0.487
	0.6	0.887	0.408
	0.7	0.837	0.340
	0.8	0.778	0.277
	0.9	0.705	0.215

TABLE 2. Comparison of the normalized velocities of a sphere moving along the axis of an orifice for a selection of the cases of electrophoresis and sedimentation shown in figure 2 (data rounded to three decimal places)

important and even stronger than the effect of viscous retardation caused by the wall for $a/b \leqslant 1$ and $a/d \to 1$.

On the other hand, if a sphere has a relatively large radius compared with that of the orifice, or if a sphere has smaller radius and is located sufficiently far from the orifice, both the electrophoretic and hydrodynamic mobilities decrease with the increase of the spacing parameter a/d. For these cases the boundary wall behaves like an infinite solid plane which enhances the viscous retardation of the particle as it tries to move in response to the applied field. The increase of the electrical driving force on the particle's surface in the gap region (if there is any), which tends to speed up the electrophoretic sphere, is not strong enough to compensate for the larger viscous drag of the wall. In fact, for the limiting case of electrophoresis of a sphere normal to an infinite plane, the wall effect on the interaction between particle and electric field will reduce rather than enhance, the particle velocity (Keh & Anderson 1985). According to figure 2 and table 2, a plot of the normalized electrophoretic mobility versus a/b at $a/d = 0.9$ would show a maximum. This maximum value appears at $a/b \approx 0.63$ and is about 2.6% higher than the Smoluchowski's result with

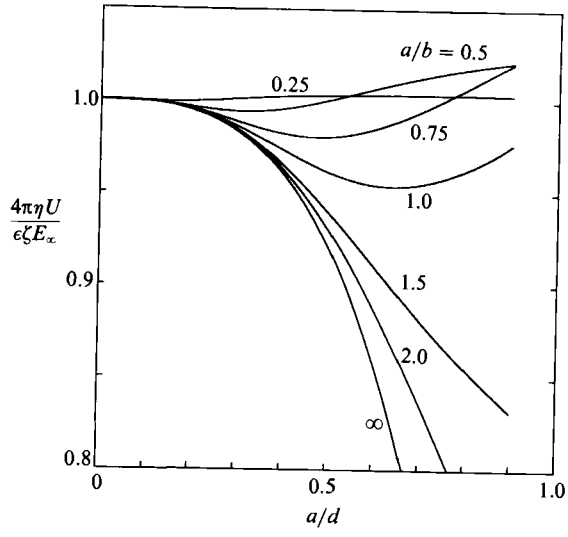

FIGURE 2. Plots of the normalized electrophoretic mobility of a sphere migrating along the axis of an orifice versus the separation variable a/d with the ratio of radii a/b as a parameter.

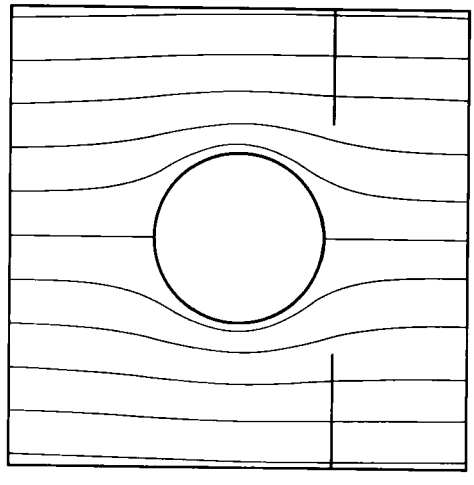

FIGURE 3. Electric field lines for the electrophoretic motion of a sphere along the axis of an orifice with $a/b = 0.75$ and $a/d = 0.9$.

the boundary being far away from the particle or for the case of $a/b \to 0$. It should be noticed that, in general, the wall effect on electrophoresis toward an orifice is much weaker than that on the corresponding motion driven by a body force, as was observed for the electrophoresis near a plane wall or inside a long pore (Keh & Anderson 1985).

The fluid flow resulting from electrophoresis is force-free and is thus irrotational. The primary disturbance caused by the particle is that of a potential doublet, in contrast to the Stokeslet dominated disturbance exhibited by a particle moving under the influence of a body force. For the electrophoretic motion of a colloidal sphere along the axis of an orifice, the stream function for the flowing fluid can be evaluated from the combination of Ψ_1 obtained by Dagan *et al.* (1982*c*) and Ψ_2 given

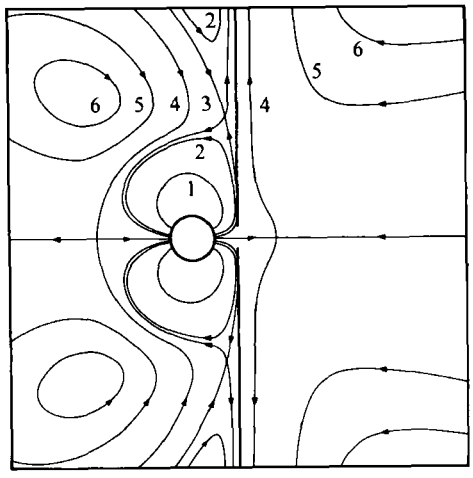

FIGURE 4. Streamlines for the electrophoretic motion of a sphere along the axis of an orifice with $a/b = 2.0$ and $a/d = 0.5$. Curve 1, $4\pi\eta\Psi/a^2\epsilon\zeta E_\infty = -0.075$; 2, -0.01; 3, -0.007825; 4, 0; 5, 0.0125; 6, 0.02.

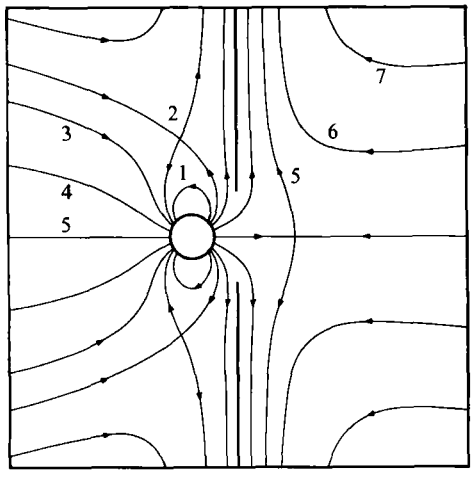

FIGURE 5. Streamlines for the electrophoretic motion of a sphere along the axis of an orifice with $a/b = 0.5$ and $a/d = 0.5$. Curve 1, $4\pi\eta\Psi/a^2\epsilon\zeta E_\infty = -0.24$; 2, -0.1734; 3, -0.12; 4, -0.04; 5, 0; 6, 0.04; 7, 0.12.

by (2.28)–(2.31) with coefficients determined by the boundary–collocation technique. The streamlines for the situation when the radius of the sphere is relatively large compared with that of the orifice are depicted in figure 4. The contour pattern illustrates the distortion of fluid recirculation around the sphere due to the orifice wall in the proximity. The existence of a toroidal 'inner' circulation pattern for electrophoresis corresponds to that of a potential dipole. In addition to the local inner recirculation region in the vicinity of the sphere, there are two toroidal 'outer' recirculation regions on the side $z < d$, swirling in opposite directions, far away from the particle. Note that the fluid flow contains a circle (around the axis) of stagnation points where the inner recirculation region and one of the two outer recirculation regions meet each other. Also, two more stagnation points, one in each half-space,

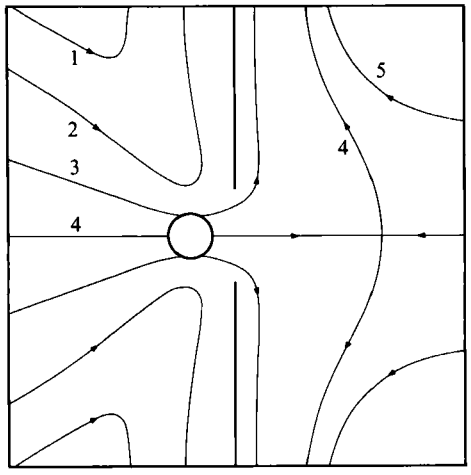

FIGURE 6. Streamlines for the sedimentation of a sphere along the axis of an orifice with $a/b = 0.5$ and $a/d = 0.5$. Curve 1, $\Psi/a^2U = -1.6$; 2, -1.2; 3, -0.4; 4, 0; 5, 0.12.

appear on the axis of the orifice. The circulating streamline $\Psi = 0$ intersects the axis at these points orthogonally. The relative position of each stagnation point with respect to the orifice depends on the ratios a/b and a/d, but is independent of the electrophoretic velocity of the particle. For the limiting case as $a/b \to \infty$ (electrophoresis normal to an infinite plane), the circle of stagnation points will shift onto the plane wall and only one outer recirculation region (instead of the two shown in figure 4) exists in a meridian plane (Keh & Lien 1989).

The streamline pattern for the case when the radius of the electrophoretic sphere is smaller than or comparable with that of the orifice is drawn in figure 5. In the half-space $z < d$, the flow still contains a circle of stagnation points, but there is only one outer recirculation region in each meridian plane and no stagnation point appears on the axis of symmetry. Note that, the direction of this outer recirculation is opposite to that for the electrophoretic motion of a sphere perpendicular to an infinite plane.

Figure 6 corresponds to the typical streamline pattern for the case of a sphere moving along the axis of an orifice driven by a body force, which can be made by obtaining Ψ_1 only. In comparison with the situations of electrophoresis toward an orifice, the presence of the boundary wall causes no inner-and-outer recirculation in the region $z < d$ for the motion under gravity. This is because the disturbance to the fluid velocity field caused by an electrophoretic sphere decays much faster than that caused by a Stokeslet. It should be noticed from figures 4–6 that the streamline pattern for the half-space $z > d$ for electrophoresis resembles that for sedimentation, and the direction of the bulk flow in the axial region is opposite to that of the movement of the particle.

4. Formulation for the electrophoretic motion of a sphere normal to a disk

The axisymmetric electrophoresis of a non-conducting sphere of radius a towards a circular disk of radius b located at a distance d from the sphere centre is considered in this section, an inverse geometry to that studied in §2. The disk is assumed to be perfectly conducting and of zero thickness. The sphere centre is chosen to be the origin of the coordinate frame, as shown in figure 7, and the uniformly applied

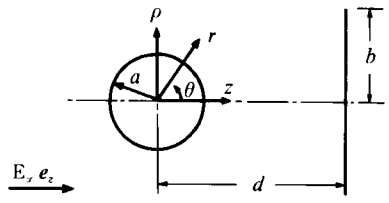

FIGURE 7. Electrophoresis of a spherical particle along the axis of a conducting circular disk of zero thickness.

electric field is expressed by $E_\infty \boldsymbol{e}_z$. The thin-double-layer assumption is employed. Our purpose here is to determine the electrophoretic velocity of the particle in the proximity of the disk.

Similar to the problem considered in §2, both the electrical potential and the fluid velocity fields outside the particle have to be solved to determine the particle velocity.

4.1. *Electrical potential distribution*

The potential field is divided into two regions, the semi-infinite space containing the sphere, $z \leqslant d$, and the remaining half-space $z \geqslant d$. Then, the solution in the forms of (2.3)–(2.6) and the boundary conditions given in (2.2*a*) and (2.2*c*) are all valid here. However, in the case of a disk at the plane $z = d$, the boundary condition (2.2*b*) should be replaced by

$$\Phi = -E_\infty d \quad \text{at} \quad z = d \text{ and } 0 \leqslant \rho \leqslant b. \tag{4.1}$$

The electrical potential at the plane of the disk is defined by

$$\Phi(\rho, d) = -E_\infty d + \frac{h(\rho)}{\rho} \quad (b < \rho < \infty). \tag{4.2}$$

Thus, mixed boundary conditions in the matching plane become

$$\Phi^{\mathrm{I}}(\rho, d) = \Phi^{\mathrm{II}}(\rho, d) = \begin{cases} -E_\infty d + h(\rho)/\rho & (b < \rho < \infty) \\ -E_\infty d & (0 \leqslant \rho \leqslant b), \end{cases} \tag{4.3}$$

$$\frac{\partial \Phi^{\mathrm{I}}}{\partial z}(\rho, d) = \frac{\partial \Phi^{\mathrm{II}}}{\partial z}(\rho, d) \quad (b < \rho < \infty). \tag{4.4}$$

Application of the boundary conditions (4.3) to the solution of Φ^{I} and Φ^{II} given by (2.3)–(2.6) and utilization of Hankel transforms provide solutions for $R_1(\omega)$ and $R_2(\omega)$ in terms of the unknown T_n and $h(\rho)$. The resulting potential field for the two regions can also be expressed by (2.10) and (2.13), with the definition of $h^*(\omega)$ in (2.11) being replaced by

$$h^*(\omega) \equiv \omega \int_b^\infty h(t)\, J_0(\omega t)\, \mathrm{d}t. \tag{4.5}$$

Substituting (2.10) and (2.13) into the matching condition (4.4), one obtains the relation

$$\int_0^\infty \omega h^*(\omega)\, J_0(\omega\rho)\, \mathrm{d}\omega = H(\rho) \quad (b < \rho < \infty), \tag{4.6}$$

where $H(\rho)$ has the same form as (2.14*b*).

Equation (4.6) together with

$$\int_0^\infty h^*(\omega)\, J_0(\omega\rho)\, \mathrm{d}\omega = 0 \quad (0 \leqslant \rho \leqslant b) \tag{4.7}$$

comprise a set of dual integral equations for $h^*(\omega)$. The solution of these dual integral equations is given by Tranter (1951):

$$h^*(\omega) = H^*(\omega) - \frac{2}{\pi}\int_0^b \mathrm{d}t \cos(\omega t) \int_0^\infty \mathrm{d}s \cos(ts)\, H^*(s), \tag{4.8}$$

where

$$H^*(\omega) \equiv \int_0^\infty tH(t)\, J_0(\omega t)\, \mathrm{d}t = \sum_{n=0}^{\infty} T_n \frac{\omega^n}{n!} \mathrm{e}^{-\omega d}. \tag{4.9}$$

Substitution of (4.9) into (4.8) yields

$$h^*(\omega) = \sum_{n=0}^{\infty} T_n \left[\frac{\omega^n}{n!}\mathrm{e}^{-\omega d} - \frac{2}{\pi}\int_0^b C_{n+1}(t,d)\cos(\omega t)\,\mathrm{d}t\right], \tag{4.10}$$

where $C_n(t,d)$ is defined by (A 19).

The electrical potential field for the two semi-infinite regions is obtained by substituting (4.10) back into (2.10) and (2.13), with the result

$$\Phi^{\mathrm{I}} = -E_\infty z + \sum_{n=0}^{\infty} T_n \left[B_n''(\rho,z) - \frac{2}{\pi}\int_0^b C_{n+1}(t,d)\, Q_0^0(\rho,z,t)\,\mathrm{d}t\right], \tag{4.11a}$$

$$\Phi^{\mathrm{II}} = -E_\infty z + \sum_{n=0}^{\infty} T_n \left[B_n''(\rho,z) - \frac{2}{\pi}\int_0^b C_{n+1}(t,d)\, Q_0^0(\rho,z,t)\,\mathrm{d}t\right], \tag{4.11b}$$

where the definition of $Q_\nu^\mu(\rho,z,t)$ is given by (A 20). The unknown coefficients T_n in (4.11) are to be determined from the remaining boundary condition (2.2*a*) on the particle surface. Note that (4.11*a*) reduces to (2.17) for the limiting case of a disk with infinite radius ($b \to \infty$).

Applying the relation (2.18) and boundary condition (2.2*a*) to (4.11*a*), one obtains

$$\sum_{n=0}^{\infty} T_n \left\{\rho A_n(\rho,z) - (n+1)\, zB_{n+1}''(\rho,z) - \frac{2}{\pi}\left[z\int_0^b C_{n+1}(t,d)\, Q_0^1(\rho,z,t)\,\mathrm{d}t - \rho\int_0^b C_{n+1}(t,d)\, Q_1^1(\rho,z,t)\,\mathrm{d}t\right]\right\} = E_\infty z \quad (r=a), \tag{4.12}$$

where $A_n(\rho,z)$ is given by (2.20). Now, the collocation technique described in §2 can be used. The infinite series in solution (4.11) and boundary condition (4.12) are truncated after N terms and the truncated form of (4.12) is applied at N discrete points along the particle surface. This generates a system of N linear algebraic equations for N unknown coefficients T_n. Once these coefficients are determined, the solution for the electrical potential field is completely known.

4.2. *Fluid velocity distribution*

For the case of the electrophoretic motion of a sphere along the axis of a disk considered in this section, (2.21)–(2.25) are still valid, except that the boundary condition (2.24*b*) is replaced by

$$\boldsymbol{v} = \boldsymbol{0} \quad \text{at} \quad z = d \text{ and } 0 \leqslant \rho \leqslant b. \tag{4.13}$$

The total fluid flow is decomposed into two parts. First, the flow caused by a sphere translating along the axis of a circular disk with velocity $U\boldsymbol{e}_z$ is considered. The Stokes equations for this flow have been solved using the boundary–collocation method by Dagan *et al.* (1982*a*) and the drag force acting on the sphere can be expressed as

$$F_1 = -6\pi\eta a U\gamma, \tag{4.14}$$

where the wall-correction factor γ is related to the ratios a/b and a/d. Next, we consider the fluid motion concerning a stationary sphere located on the axis of a disk with a tangential electrokinetic velocity given by (2.27) at the particle surface. Superimposing this velocity field with that caused by a sphere translating along the axis of a disk yields the total velocity field produced by the corresponding electrophoretic motion. By obtaining an expression for the force exerted on the stationary sphere, adding it to the force given by (4.14) and equating the sum to zero, the wall-corrected electrophoretic velocity of the particle will result.

Again, we divide the flow field about the stationary sphere with a tangential velocity distribution at the surface into two semi-infinite regions. The plane of the disk, $z = d$, is the interface between the two regions. The solution in the forms (2.28)–(2.31) are also valid here. The velocity components at the plane of the disk are defined by

$$\left.\begin{aligned} v_{2z}(\rho, d) &= f(\rho)/\rho \\ v_{2\rho}(\rho, d) &= -g(\rho)/\rho \end{aligned}\right\} \quad (b < \rho < \infty). \tag{4.15}$$

Consequently, the kinematic boundary conditions in the matching plane $z = d$ become

$$v_{2z}^{\mathrm{I}}(\rho, d) = v_{2z}^{\mathrm{II}}(\rho, d) = \begin{cases} 0 & (0 \leqslant \rho \leqslant b) \\ f(\rho)/\rho & (b < \rho < \infty), \end{cases} \tag{4.16a}$$

$$v_{2\rho}^{\mathrm{I}}(\rho, d) = v_{2\rho}^{\mathrm{II}}(\rho, d) = \begin{cases} 0 & (0 \leqslant \rho \leqslant b) \\ -g(\rho)/\rho & (b < \rho < \infty). \end{cases} \tag{4.16b}$$

The dynamic matching conditions are still given by (2.34), but now for $\rho > b$.

Application of conditions (4.16) and (2.34) to (2.28)–(2.31) leads to solutions for the unknown functions $X_1(\omega)$, $Y_1(\omega), X_2(\omega)$, $Y_2(\omega), f(\rho)$ and $g(\rho)$ in terms of the unknown coefficients B_n and D_n. These results are substituted back into (2.28)–(2.30) and the velocity field for the half-space $z \leqslant d$ can be obtained, after considerable algebraic manipulation, in the form (Dagan *et al.* 1982*a*)

$$v_{2\rho}^{\mathrm{I}} = \sum_{n=2}^{\infty} \left\{ B_n \left[B_n'(\rho, z) - \frac{2}{\pi} \int_0^b B_n^*(\rho, z, t)\, \mathrm{d}t \right] + D_n \left[D_n'(\rho, z) - \frac{2}{\pi} \int_0^b D_n^*(\rho, z, t)\, \mathrm{d}t \right] \right\}, \tag{4.17a}$$

$$v_{2z}^{\mathrm{I}} = \sum_{n=2}^{\infty} \left\{ B_n \left[B_n''(\rho, z) - \frac{2}{\pi} \int_0^b B_n^{**}(\rho, z, t)\, \mathrm{d}t \right] + D_n \left[D_n''(\rho, z) - \frac{2}{\pi} \int_0^b D_n^{**}(\rho, z, t)\, \mathrm{d}t \right] \right\}. \tag{4.17b}$$

Here, the functions B_n', B_n'', D_n', D_n'', B_n^*, B_n^{**}, D_n^* and D_n^{**} are defined by (A 5)–(A 8) and (A 15)–(A 20). Similarly, the velocity components for the other half-space are

$$\begin{aligned} v_{2\rho}^{\mathrm{II}} = \sum_{n=2}^{\infty} \Bigg\{ & B_n \left[B_n'(\rho, z) - \frac{2}{\pi} \int_0^b B_n^*(\rho, z, t)\, \mathrm{d}t \right] \\ & + D_n \left[\frac{2n-3}{n} z B_{n-1}'(\rho, z) - \frac{n-2}{n-1} B_{n-2}'(\rho, z) - \frac{2}{\pi} \int_0^b D_n^*(\rho, z, t)\, \mathrm{d}t \right] \Bigg\}, \end{aligned} \tag{4.17c}$$

$$\begin{aligned} v_{2z}^{\mathrm{II}} = \sum_{n=2}^{\infty} \Bigg\{ & B_n \left[B_n''(\rho, z) - \frac{2}{\pi} \int_0^b B_n^{**}(\rho, z, t)\, \mathrm{d}t \right] \\ & + D_n \left[\frac{2n-3}{n} z B_{n-1}''(\rho, z) - \frac{n-3}{n} B_{n-2}''(\rho, z) - \frac{2}{\pi} \int_0^b D_n^{**}(\rho, z, t)\, \mathrm{d}t \right] \Bigg\}. \end{aligned} \tag{4.17d}$$

$\frac{a}{d}$	$\frac{4\pi\eta U}{\epsilon\zeta E_\infty}$		
	$a/b = 0$	$a/b = 0.1$	$a/b = 0.25$
0.1	0.99938	0.99929	0.99910
0.2	0.99504	0.99508	0.99371
0.3	0.98330	0.98339	0.98229
0.4	0.96020	0.96029	0.96012
0.5	0.92089	0.92099	0.92156
0.6	0.85862	0.85872	0.85974
0.7	0.76297	0.76298	0.76424
0.8	0.61631	0.60300	0.61749

TABLE 3. The normalized electrophoretic mobilities for the motion of a sphere along the axis of a circular disk with the ratio of radii $a/b = 0$, 0.1, and 0.25

For the limiting case of a disk with infinite radius, the resulting solution for the velocity field in the region $z \leqslant d$ is identical to that given by (2.37).

The unknown coefficients B_n and D_n in (4.17) are to be determined from the boundary condition on the particle surface. Substitution of (4.11*a*) into (2.27) provides the tangential velocity components at the particle 'surface'

$$v_{2\rho}|_{r=a} = \frac{\epsilon\zeta}{4\pi\eta}\sum_{n=0}^{\infty} T_n\left[A_n(\rho,z)+\frac{2}{\pi}\int_0^b C_{n+1}(t,d)\,Q_1^1(\rho,z,t)\,\mathrm{d}t\right], \tag{4.18a}$$

$$v_{2z}|_{r=a} = -\frac{\epsilon\zeta}{4\pi\eta}E_\infty - \frac{\epsilon\zeta}{4\pi\eta}\sum_{n=0}^{\infty} T_n\left[(n+1)B''_{n+1}(\rho,z)+\frac{2}{\pi}\int_0^b C_{n+1}(t,d)\,Q_0^1(\rho,z,t)\,\mathrm{d}t\right]. \tag{4.18b}$$

To use the collocation technique, the infinite series in (4.17) are truncated after M terms and the boundary conditions (4.18) (in which the coefficients T_n are determined through the procedure given by §4.1) are applied at M discrete points along the surface of the sphere. The resulting system of $2M$ linear algebraic equations can be solved to yield the $2M$ unknown coefficients B_n and D_n. The velocity field is completely determined once these coefficients are obtained. Note that the drag exerted by the fluid on the sphere is still given by (2.40).

4.3. *Derivation of the particle velocity*

The net force acting on the electrophoretic particle, which is the combination of the two forces given by (4.14) and (2.40), must vanish. This restraint results in the electrophoretic velocity of the particle

$$U = \frac{2D_2}{3a\gamma}. \tag{4.19}$$

5. Solutions for the electrophoresis of a sphere normal to a disk

In §3 collocation solutions for the electrophoretic motion of a non-conducting sphere along the axis of orifice have been presented and were shown to be in perfect agreement with the exact solutions for the limiting case. This section will examine

$\frac{a}{b}$	$\frac{a}{d}$	Electrophoresis $\frac{4\pi\eta U}{\epsilon\zeta E_\infty}$	Sedimentation $\frac{6\pi\eta aU}{F}$
0.5	0.1	0.9994	0.947
	0.2	0.993	0.823
	0.3	0.976	0.686
	0.4	0.950	0.564
	0.5	0.911	0.459
	0.6	0.852	0.364
	0.7	0.762	0.274
	0.8	0.620	0.185
	0.9	0.391	0.095
1.0	0.1	0.9997	0.972
	0.2	0.995	0.896
	0.3	0.978	0.786
	0.4	0.942	0.660
	0.5	0.884	0.528
	0.6	0.801	0.402
	0.7	0.693	0.288
	0.8	0.552	0.186
	0.9	0.349	0.093
5.0	0.1	0.99993	0.994
	0.2	0.9989	0.978
	0.3	0.995	0.952
	0.4	0.983	0.920
	0.5	0.959	0.881
	0.6	0.913	0.833
	0.7	0.824	0.764
	0.8	0.631	0.637
	0.9	0.193	0.364

TABLE 4. Comparison of the normalized velocities of a sphere moving along the axis of a circular disk for a selection of the cases of electrophoresis and sedimentation shown in figure 8 (rounded to three decimal places)

the solutions for the axisymmetric electrophoretic motion of a sphere toward a circular disk using the same collocation method. The system of linear algebraic equations to be solved for T_n is constructed from (4.11a) and (4.12), and that for B_n and D_n is provided by (4.17a, b) and (4.18).

In table 3, numerical solutions of the wall-corrected electrophoretic mobility for a sphere migrating along the axis of a large disk are presented. These solutions converge to at least five significant figures for all the given values of a/d (up to 0.8). It can be seen that the results for a sphere with a radius one tenth as large as that of the disk ($a/b = 0.1$) agree quite well with those for a sphere undergoing electrophoresis perpendicular to an infinitely large disk ($a/b = 0$). Even for a sphere with $a/b = 0.25$, its electrophoretic mobility differs less than 0.2% from that for the case $a/b = 0$.

The numerical results for the normalized electrophoretic velocity of a sphere migrating toward a disk with various values of a/b and a/d are shown in the first three columns of table 4 and depicted in figure 8. The Stokes-law correction for a sphere in the same geometrical system was obtained by Dagan *et al.* (1982a) and the corresponding results are computed and listed in the last column of table 4 for

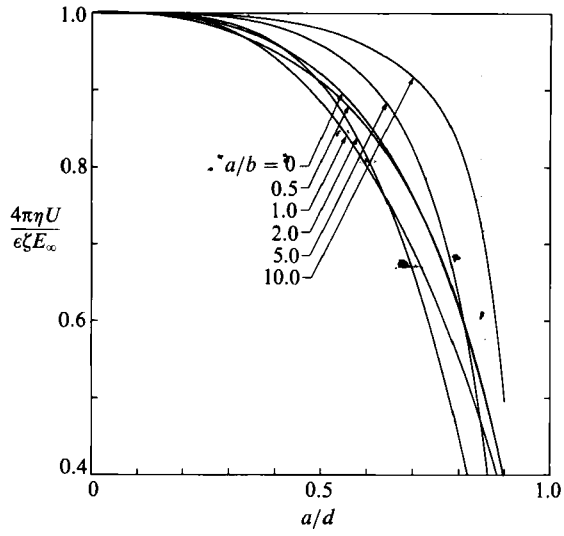

FIGURE 8. Plots of the normalized electrophoretic mobility of a sphere migrating along the axis of a circular disk versus the separation variable a/d with the ratio of radii a/b as a parameter.

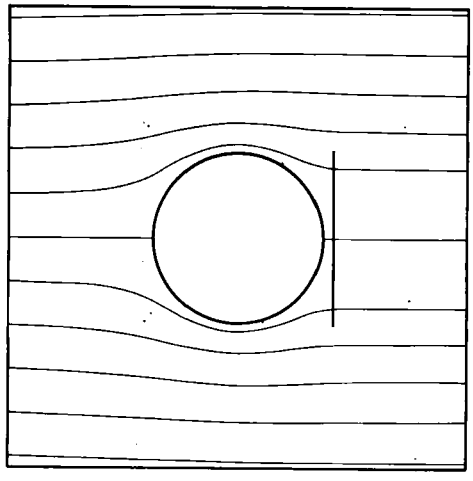

FIGURE 9. Electric field lines for the electrophoretic motion of a sphere along the axis of a circular disk with $a/b = 1.0$ and $a/d = 0.9$.

comparison. An interesting feature is observed in tables 3 and 4 and figure 8: for a sphere close to a circular disk of a comparable or larger radius, both its electrophoretic and hydrodynamic mobilities can be lower than those for a sphere translating toward an infinite plane wall. These results reflect the fact that the sharp edge and back surface of a finite disk introduce a strong resistance to the fluid motion caused by a migrating particle and this resistance can be greater than that produced by the additional surface of an infinite wall. No matter what the ratio of sphere-to-disk radii is, both of the electrophoretic and hydrodynamic mobilities decrease steadily as the particle approaches the disk wall (with increasing a/d), going to zero at the limit. The wall effect on electrophoresis toward a disk in general is also much weaker than that for sedimentation, an exception being the case when both a/b and a/d are large (in

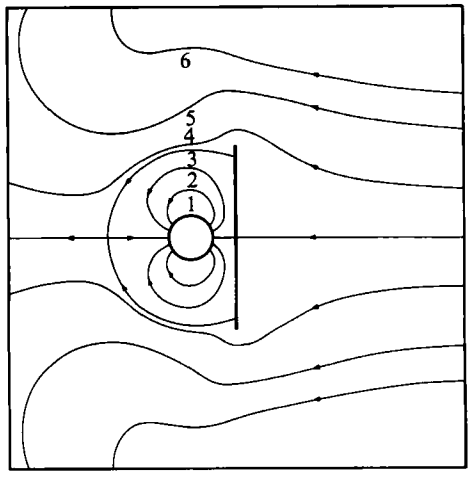

FIGURE 10. Streamlines for the electrophoretic motion of a sphere along the axis of a circular disk with $a/b = 0.25$ and $a/d = 0.5$. Curve 1, $4\pi\eta\Psi/a^2\epsilon\zeta E_\infty = -0.14$; 2, -0.04; 3, 0; 4, 0.008; 5, 0.04; 6, 0.07.

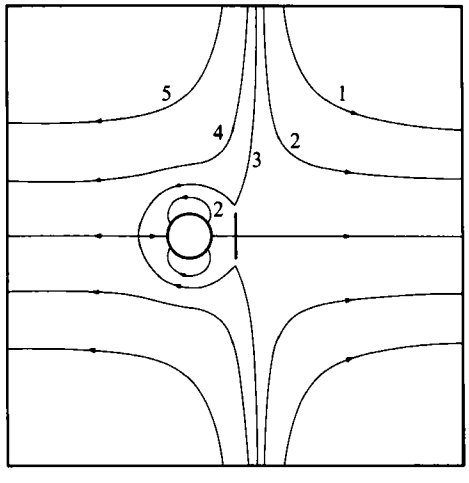

FIGURE 11. Streamlines for the electrophoretic motion of a sphere along the axis of a circular disk with $a/b = 1.0$ and $a/d = 0.5$. Curve 1, $4\pi\eta\Psi/a^2\epsilon\zeta E_\infty = -0.5$; 2, -0.15; 3, 0; 4, 0.2; 5, 0.8.

which the wall effect on the interaction between particle and electric field is to decrease the particle velocity significantly). As a comparison to figure 3, the electric field lines for the case of a disk with $a/b = 1.0$ and $a/d = 0.9$ are drawn in figure 9. The local electric field at the sphere 'surface' on the near side to the disk is depressed compared with that on the far side. This demonstrates that the effect of the disk on the interaction between particle and electric field will reduce the electrophoretic velocity of the particle.

The streamline pattern for the electrophoretic motion of an insulating sphere along the axis of a conducting disk with a larger radius is drawn in figure 10. In addition to the local 'inner' recirculation around the sphere, there is an 'outer' recirculation extending to the whole remaining fluid phase. The direction of this outer recirculation in the axial region is opposite to that of the particle's movement.

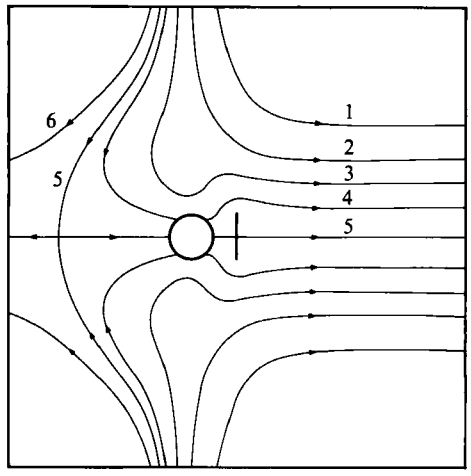

FIGURE 12. Streamlines for the sedimentation of a sphere along the axis of a circular disk with $a/b = 1.0$ and $a/d = 0.5$. Curve 1, $\Psi/a^2U = -4.0$; 2, -2.0; 3, -1.0; 4, -0.3; 5, 0; 6, 0.5.

For the electrophoretic motion of a sphere whose radius is larger than or comparable with that of the disk, the distortion of the flow field due to the presence of the disk is illustrated in figure 11. In each meridian plane, two outer recirculation regions that swirl in opposite directions appear. Compared to the case shown in figure 10 for a larger disk, there is no stagnation point on the disk other than its centre in figure 11. Also, the direction of axial flow in the region $z \geqslant d$ is the same as that of the electrophoresis.

In figure 12, the situation for a sphere sedimenting along the axis of a disk is considered. Contrary to the streamline patterns for electrophoresis, there is no inner-and-outer recirculation or stagnation point on the disk other than its centre in the fluid motion, no matter what the ratio a/b is. Note that there is a stagnation point on the axis in the region $z < d$, similar to the situations of electrophoresis shown in figures 10 and 11.

6. Concluding remarks

The electrophoresis of colloidal spheres approaching a perfectly conducting solid surface is often encountered in the electrophoretic deposition of dielectric materials. It is important to understand if the solid surface significantly affects the movement of the spheres. In this work, the solutions for the axisymmetric, electrophoretic motion of a spherical particle with a thin electrical double layer normal to a conducting plane with a circular orifice and normal to a conducting disk have been obtained. In the limit of a small orifice and a large disk, our solutions agree very well with the exact solution for the electrophoretic motion of a sphere normal to an infinite conducting plane. Some interesting results which differ significantly from those of the corresponding sedimentation problem have emerged. The electrophoretic mobility for a particle approaching an orifice larger than the particle diameter can be enhanced, owing to the feature of squeezed electric field lines in the gap between the particle and the orifice edge. On the other hand, the mobility for a particle undergoing electrophoresis toward a disk can be reduced significantly, because the

wall effect on the interaction between particle and electric field in this situation is to decrease the particle velocity. The Stokes stream function for the fluid flow in four representative cases of electrophoresis has been presented in figures 4, 5, 10 and 11, while the streamline pattern for the corresponding cases of sedimentation is shown in figures 6 and 12 for comparison. Both figures 4 and 5 show the remarkable feature that the flow field for the electrophoresis of a sphere toward an orifice contains a circle of stagnation points.

In addition to the electrophoretic deposition, another scientific application of the electrophoretic motion of particles toward an orifice occurs in a Coulter counter designed not only to count and size particles but also to determine their zeta potentials (DeBlois & Bean 1970). In spite of the fact that the Coulter counter employs an insulating plane with an orifice, not the conducting plane assumed here, our solution method may still be used to solve the problem after the boundary conditions at the plane of the orifice have been properly modified. Also, in practical applications of electrophoresis, the particles can approach an orifice or a disk on an off-centre path. It would be of interest to know if the hydrodynamic and electrostatic forces tend to push the particle more off-centre or to bring it back to the centreline. This asymmetric problem is now under investigation and will be presented in a subsequent article.

This research was supported by the National Science Council of the Republic of China.

Appendix

For conciseness the definitions of some functions in §§2 and 4 are listed here. It should be noted that there are several typographical errors in the original formulae given by Dagan *et al.* (1982*a*, *c*).

$$\beta'_n(\rho,z) = B'_n(\rho,z) - B'_n(\rho,2d-z) + 2(n+1)(d-z)B'_{n+1}(\rho,2d-z), \tag{A 1}$$

$$\delta'_n(\rho,z) = D'_n(\rho,z) - D'_n(\rho,2d-z) - (2/n)(n-1)(n-3)(d-z)B'_{n-1}(\rho,2d-z) + 2(2n-3)d(d-z)B'_n(\rho,2d-z), \tag{A 2}$$

$$\beta''_n(\rho,z) = B''_n(\rho,z) - B''_n(\rho,2d-z) - 2(n+1)(d-z)B''_{n+1}(\rho,2d-z), \tag{A 3}$$

$$\delta''_n(\rho,z) = D''_n(\rho,z) - D''_n(\rho,2d-z) + 2(n-2)(d-z)B''_{n-1}(\rho,2d-z) - 2(2n-3)d(d-z)B''_n(\rho,2d-z), \tag{A 4}$$

where

$$B'_n(\rho,z) = \frac{n+1}{\rho(\rho^2+z^2)^{\frac{1}{2}n}} G_{n+1}^{-\frac{1}{2}}\left[\frac{z}{(\rho^2+z^2)^{\frac{1}{2}}}\right], \tag{A 5}$$

$$D'_n(\rho,z) = \frac{n+1}{\rho(\rho^2+z^2)^{\frac{1}{2}(n-2)}} G_{n+1}^{-\frac{1}{2}}\left[\frac{z}{(\rho^2+z^2)^{\frac{1}{2}}}\right] - \frac{2z}{\rho(\rho^2+z^2)^{\frac{1}{2}(n-1)}} G_n^{-\frac{1}{2}}\left[\frac{z}{(\rho^2+z^2)^{\frac{1}{2}}}\right], \tag{A 6}$$

$$B''_n(\rho,z) = \frac{1}{(\rho^2+z^2)^{\frac{1}{2}(n+1)}} P_n\left[\frac{z}{(\rho^2+z^2)^{\frac{1}{2}}}\right], \tag{A 7}$$

$$D''_n(\rho,z) = \frac{2}{(\rho^2+z^2)^{\frac{1}{2}(n-1)}} G_n^{-\frac{1}{2}}\left[\frac{z}{(\rho^2+z^2)^{\frac{1}{2}}}\right] + \frac{1}{(\rho^2+z^2)^{\frac{1}{2}(n-1)}} P_n\left[\frac{z}{(\rho^2+z^2)^{\frac{1}{2}}}\right]. \tag{A 8}$$

P_n is the Legendre polynomial of order n, and $G_n^{-\frac{1}{2}}$ is the Gegenbauer polynomial of the first kind of order n and degree $-\frac{1}{2}$.

$$\beta_n^*(\rho,z,t) = (n+1)\,S_{n+2}(t,d)\,[K_1^{-1}(\rho,z,t) - |d-z|K_1^0(\rho,z,t)] - (d-z)\,S_{n+1}(t,d)\,K_1^1(\rho,z,t), \tag{A 9}$$

$$\delta_n^*(\rho,z,t) = [(2n-3)\,dS_{n+1}(t,d) - (n-2)\,S_n(t,d)]\,[K_1^{-1}(\rho,z,t) - |d-z|K_1^0(\rho,z,t)]$$
$$-(1/n)\,(d-z)\,[(2n-3)\,dS_n(t,d) - (n-3)\,S_{n-1}(t,d)]\,K_1^1(\rho,z,t), \tag{A 10}$$

$$\beta_n^{**}(\rho,z,t) = S_{n+1}(t,d)\,[K_0^0(\rho,z,t) + |d-z|K_0^1(\rho,z,t)] + (n+1)\,(d-z)\,S_{n+2}(t,d)\,K_0^0(\rho,z,t), \tag{A 11}$$

$$\delta_n^{**}(\rho,z,t) = (1/n)\,[(2n-3)\,dS_n(t,d) - (n-3)\,S_{n-1}(t,d)]\,[K_0^0(\rho,z,t)$$
$$+|d-z|K_0^1(\rho,z,t)] + (d-z)\,[(2n-3)\,dS_{n+1}(t,d) - (n-2)\,S_n(t,d)]\,K_0^0(\rho,z,t), \tag{A 12}$$

where
$$S_n(t,d) = \frac{1}{(t^2+d^2)^{\frac{1}{2}n}} \sin\left[n \tan^{-1}\left(\frac{t}{d}\right)\right], \tag{A 13}$$

$$K_\nu^\mu(\rho,z,t) = \int_0^\infty \omega^\mu J_\nu(\omega\rho)\,\mathrm{e}^{-\omega|d-z|} \sin(\omega t)\,\mathrm{d}\omega, \tag{A 14}$$

and J_ν is the Bessel function of the first kind of order ν.

$$B_n^*(\rho,z,t) = (n+1)\,C_{n+2}(t,d)\,[Q_1^{-1}(\rho,z,t) - |d-z|Q_1^0(\rho,z,t)] - (d-z)\,C_{n+1}(t,d)\,Q_1^1(\rho,z,t), \tag{A 15}$$

$$D_n^*(\rho,z,t) = [(2n-3)\,dC_{n+1}(t,d) - (n-2)\,C_n(t,d)]\,[Q_1^{-1}(\rho,z,t) - |d-z|Q_1^0(\rho,z,t)]$$
$$-(1/n)\,(d-z)\,[(2n-3)\,dC_n(t,d) - (n-3)\,C_{n-1}(t,d)]\,Q_1^1(\rho,z,t), \tag{A 16}$$

$$B_n^{**}(\rho,z,t) = C_{n+1}(t,d)\,[Q_0^0(\rho,z,t) + |d-z|Q_0^1(\rho,z,t)] + (n+1)\,(d-z)\,C_{n+2}(t,d)\,Q_0^0(\rho,z,t), \tag{A 17}$$

$$D_n^{**}(\rho,z,t) = (1/n)\,[(2n-3)\,dC_n(t,d) - (n-3)\,C_{n-1}(t,d)]\,[Q_0^0(\rho,z,t)$$
$$+|d-z|Q_0^1(\rho,z,t)] + (d-z)\,[(2n-3)\,dC_{n+1}(t,d) - (n-2)\,C_n(t,d)]\,Q_0^0(\rho,z,t), \tag{A 18}$$

where
$$C_n(t,d) = \frac{1}{(t^2+d^2)^{\frac{1}{2}n}} \cos\left[n \tan^{-1}\left(\frac{t}{d}\right)\right], \tag{A 19}$$

$$Q_\nu^\mu(\rho,z,t) = \int_0^\infty \omega^\mu J_\nu(\omega\rho)\,\mathrm{e}^{-\omega|d-z|} \cos(\omega t)\,\mathrm{d}\omega. \tag{A 20}$$

The integral defined by (A 14) and (A 20) can be evaluated by the following formulae:

$$K_1^{-1}(\rho,z,t) = \frac{t-x}{\rho}, \quad K_1^0(\rho,z,t) = |d-z|\frac{t^2-x^2}{\rho x\sigma}, \tag{A 21 a, b}$$

$$K_1^1(\rho,z,t) = \frac{t^2-x^2}{\rho x\sigma^2}\left\{(d-z)^2\left[4+(t^2-x^2)\left(\frac{4}{\sigma}+\frac{1}{x^2}\right)\right]-\sigma\right\}, \quad K_0^0(\rho,z,t) = \frac{x}{\sigma}, \tag{A 21 c, d}$$

$$K_0^1(\rho,z,t)=\frac{|d-z|}{\sigma^3 x}[4x^2(t^2-x^2)-\sigma(t^2-3x^2)], \tag{A 21e}$$

$$Q_1^{-1}(\rho,z,t)=\frac{y-|d-z|}{\rho}, \quad Q_1^0(\rho,z,t)=\frac{1}{\rho}-|d-z|\frac{t^2+y^2}{\rho y\sigma}, \tag{A 22a, b}$$

$$Q_1^1(\rho,z,t)=\frac{t^2+y^2}{\rho y\sigma^2}\left\{(d-z)^2\left[4-(t^2+y^2)\left(\frac{4}{\sigma}+\frac{1}{y^2}\right)\right]+\sigma\right\}, \tag{A 22c}$$

$$Q_0^0(\rho,z,t)=\frac{y}{\sigma}, \quad Q_0^1(\rho,z,t)=\frac{|d-z|}{\sigma^3 y}[4y^2(t^2+y^2)-\sigma(t^2+3y^2)], \tag{A 22d, e}$$

where x and y are the positive roots of the algebraic equations

$$x^4+[(d-z)^2+\rho^2-t^2]x^2-t^2(d-z)^2=0, \tag{A 23}$$

$$y^4-[(d-z)^2+\rho^2-t^2]y^2-t^2(d-z)^2=0, \tag{A 24}$$

and σ is defined by

$$\sigma=\{[(d-z)^2+\rho^2-t^2]^2+4t^2(d-z)^2\}^{\frac{1}{2}}. \tag{A 25}$$

REFERENCES

Acrivos, A., Jeffrey, D. J. & Saville, D. A. 1990 Particle migration in suspensions by thermocapillary or electrophoretic motion. *J. Fluid Mech.* **212**, 95.

Anderson, J. L. 1981 Concentration dependence of electrophoretic mobility. *J. Colloid Interface Sci.* **82**, 248.

Anderson, J. L. 1989 Colloid transport by interfacial forces. *Ann. Rev. Fluid Mech.* **21**, 61.

Batchelor, G. K. 1972 Sedimentation in a dilute dispersion of spheres. *J. Fluid Mech.* **52**, 245.

Chen, S. B. & Keh, H. J. 1988 Electrophoresis in a dilute dispersion of colloidal spheres. *AIChE J.* **34**, 1075.

Dagan, Z., Pfeffer, R. & Weinbaum, S. 1982*a* Axisymmetric stagnation flow of a spherical particle near a finite planar surface at zero Reynolds number. *J. Fluid Mech.* **122**, 273.

Dagan, Z., Weinbaum, S. & Pfeffer, R. 1982*b* An infinite-series solution for the creeping motion through an orifice of finite length. *J. Fluid Mech.* **115**, 505.

Dagan, Z., Weinbaum, S. & Pfeffer, R. 1982*c* General theory for the creeping motion of a finite sphere along the axis of a circular orifice. *J. Fluid Mech.* **117**, 143.

Davis, A. M. J., O'Neill, M. E. & Brenner, H. 1981 Axisymmetric Stokes flow due to a rotlet and Stokeslet near a hole in a plane wall: filtration flows. *J. Fluid Mech.* **103**, 183.

DeBlois, R. W. & Bean, C. P. 1970 Counting and sizing of submicron particles by the resistive pulse technique. *Rev. Sci. Instrum.* **41**, 909.

Gluckman, M. J., Pfeffer, R. & Weinbaum, S. 1971 A new technique for treating multiparticle slow viscous flow: axisymmetric flow past spheres and spheroids. *J. Fluid Mech.* **50**, 705.

Happel, J. & Brenner, H. 1983 *Low Reynolds Number Hydrodynamics.* Martinus Nijhoff.

Hunter, R. J. 1987 *Foundations of Colloid Science*, Vol. I, p. 557. Clarendon.

Keh, H. J. & Anderson, J. L. 1985 Boundary effects on electrophoretic motion of colloidal spheres. *J. Fluid Mech.* **153**, 417.

Keh, H. J. & Chen, S. B. 1988 Electrophoresis of a colloidal sphere parallel to a dielectric plane. *J. Fluid Mech.* **194**, 377.

Keh, H. J. & Chen, S. B. 1989*a* Particle interactions in electrophoresis – I. Motion of two spheres along their line of centers. *J. Colloid Interface Sci.* **130**, 542.

Keh, H. J. & Chen, S. B. 1989*b* Particle interactions in electrophoresis – II. Motion of two spheres normal to their line of centers. *J. Colloid Interface Sci.* **130**, 556.

Keh, H. J. & Lien, L. C. 1989 Electrophoresis of a dielectric sphere normal to a large conducting plane. *J. Chinese Inst. Chem. Engng* **20**, 283.

KEH, H. J. & YANG, F. R. 1990 Particle interactions in electrophoresis – III. Axisymmetric motion of multiple spheres. *J. Colloid Interface Sci.* (in press).

KOZAK, M. W. & DAVIS, E. J. 1989 Electrokinetics of concentrated suspensions and porous media – I. Thin electrical double layers. *J. Colloid Interface Sci.* **127**, 497.

MORRISON, F. A. 1970 Electrophoresis of a particle of arbitrary shape. *J. Colloid Interface Sci.* **34**, 210.

MORRISON, F. A. & STUKEL, J. J. 1970 Electrophoresis of an insulating sphere normal to a conducting plane. *J. Colloid Interface Sci.* **33**, 88.

O'BRIEN, V. 1968 Form factors for deformed spheroids in Stokes flow. *AIChE J.* **14**, 870.

REED, C. C. & ANDERSON, J. L. 1980 Hindered settling of a suspension at low Reynolds number. *AIChE J.* **26**, 816.

REED, L. D. & MORRISON, F. A. 1976 Hydrodynamic interactions in electrophoresis. *J. Colloid Interface Sci.* **54**, 117.

TRANTER, C. J. 1951 On some dual integral equations. *Q. J. Maths* **2**, 60.